

**Formulation of a Simplified Model
of Rotor-Horizontal Stabilizer Interactions
and
Comparison with Experimental Measurements**

S. Weinstock

Office National d'Etudes et de Recherches Aéronautiques
BP 72
92322 Châtillon Cedex
France

Abstract

The aerodynamic interactions of the rotor wake on the horizontal stabilizer can affect strongly the longitudinal dynamics of an helicopter. A good representation of this phenomenon is necessary for helicopter flight mechanics simulation models. A simple rotor wake model using vortex rings is developed in order to calculate these interactions. The results of this model are compared with the experimental measurements conducted at the ONERA S2-Ch wind tunnel on a motorized helicopter scaled model.

Notations

		<i>units</i>
R	: rotor radius	mm
Ω	: rotor rotational velocity	rad/s
ΩR	: blade tip speed	m/s
n_b	: number of blades	--
c	: blade airfoil chord	mm
σ	: rotor solidity	--
$\mu, \vec{\mu}$: advance ratio, airspeed vector	--
T, m_h	: rotor thrust, helicopter equivalent mass (T/g)	N, kg
α_d	: rotor disc angle of attack	deg
χ	: rotor wake angle	deg
$\vec{\lambda}_i$: induced velocity vector	--
$\lambda_{io}, \lambda_{ic}, \lambda_{is}$: first coefficients of the Fourier expansion of the induced downwash on the rotor disc	--
Γ	: circulation	
$\Delta\alpha, \Delta\mu$: airflow deflection and airspeed variation	deg, --
N_a	: number of vortex rings	--

All the velocities, circulations and lengths are given in adimensionnal form. The velocities are divided by the tip speed ΩR , the circulations by ΩR^2 and the lengths by the rotor radius R.

Introduction

This paper presents the development of a simple rotor wake model which can be easily integrated in an helicopter flight mechanics simulation model. This model is useful to obtain a realistic representation of the rotor-horizontal stabilizer interactions which can affect strongly the longitudinal dynamics of the helicopter. Airflow deflections induced by the main rotor on the empennage are indeed far from being negligible and can reach 20 degrees. Such an interaction model could be also useful to study problems like the determination of flight path deviations of armaments fired from an helicopter.

Why is a "simple" model required ? If accurate numerical models using fixed or free wake geometries exist, their integration in a flight mechanics model is not really thinkable because they require a too important computation time and thus are not suitable for real-time simulation. Moreover, most of existing flight mechanics models use simple induced flow models like the Glauert, Mejer-Drees or Pitt and Peters models [1,2,3], rather than complex numerical ones for the calculation of rotor aerodynamic loads. Thus, it is not reasonable to use a wake model for the computation of the stabilizer loads which is much more complex than the one used for the calculation of the rotor loads.

In the first part of this paper, we will describe the rotor-horizontal stabilizer interactions experimental measurements made at the ONERA S2-Ch wind tunnel on an motorized helicopter scaled model. The analysis of these measurements will allow us to justify the use of an isolated rotor wake model for the calculation of these interactions by neglecting all other interactions, in particular the effects due to the fuselage.

The second part will describe a vortex rings model that we have developed for the computation of these interactions.

In the last part, we will compare our model with the experimental results.

1) Rotor - horizontal stabilizer interactions measurements

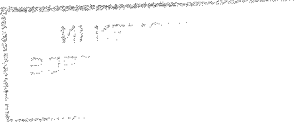
Tests were made at ONERA S2-Ch wind tunnel on an helicopter motorized scaled model.

The experiments were divided in two parts. The first part aimed at the measurement of the velocity field around the fuselage for a single aerodynamic configuration. The second part in which we are interested here, aimed at the accurate measurement of the induced velocity field in the vicinity of the empennage, for several advance ratios and for several rotor loads.

The model was an AS Dauphin II at the scale of 1/7.7. The rotor is driven by an electric motor. The characteristics of the model are :

Rotor radius :	$R = 750 \text{ mm}$
Blade tip speed:	$\Omega R = 100 \text{ m/s}$
Number of blades:	$n_b = 4$
Airfoil chord:	$c = 50 \text{ mm}$
Solidity:	$\sigma = 0.0849$

A six components external balance gave the helicopter global loads. The three velocity components were measured by laser velocimetry. The detected particles were classified according to the azimuth of a reference blade at the instant of detection. They were collected in 45 classes of 2 degrees width modulo 90 degrees (the four blades were assumed to have the same effects on the airflow). This large number of classes was necessary in order to obtain a good accuracy on the average value of the velocities.



The tests were made for four advance ratios $\mu=0.15, 0.20, 0.25$ and 0.30 with a simulated helicopter mass equal to 4 tons, and for three helicopter masses $m_h=3, 4$ and 5 tons with an advance ratio of 0.20 . The fuselage angle of attack was always at -3 degrees.

For the tests, the horizontal stabilizer was removed. The velocities were measured at six points uniformly distributed on the left half-empennage quarter-chord axis (see figure 1,2) :

point n°	x	y	z
1	0,846	0,090	0,309
2	0,846	0,127	0,309
3	0,846	0,163	0,309
5	0,846	0,200	0,309
5	0,846	0,237	0,309
6	0,846	0,273	0,309

To evaluate the importance of the interactions other than the rotor-horizontal stabilizer ones, tests were made with and without the rotor (by simply removing the blades).

The results are shown on the figures 9 to 20. Three remarks can be made :

- The induced velocities are small compared to the helicopter speed. The rotor induces mainly downwash which is far from being negligible : airflow deflections vary indeed from 4 to 20 degrees. Thus afterwards, we will concentrate mainly on the airflow deflection angle.

- As the empennage is located far from the cabin, the fuselage has a small influence on the horizontal stabilizer. This observation is confirmed by other tests like those made by Leishman [5]. So afterwards, we will neglect all the effects other than those due to the rotor. This will allow us to use an isolated rotor model.

- The variations of the induced velocities along the stabilizer span are small, except at low speed and at stations very close to the fuselage. This is due to the small dimensions of the empennage. Thus, to integrate our interaction model in an existing simulation model, we will just have to add a module which computes the downwash due to the rotor at the center of the empennage, combines it with the airflow speed, before computing the stabilizer aerodynamic loads.

2) Modelisation

At the time of our first attempts, we have tried to use classical models like the Mejer-Drees or Glauert - Coleman models [3]. These models assume that there is an infinite number of blades, a lightly loaded rotor and only tip vortices which form an elliptical cylinder with a constant or sinusoidal circulation. The comparison with the experimental results was not really good. That is the reason why we have developed a new model. Our model is directly inspired from the previous ones. The main difference is that we take into account the real number of blades.

We will assume that the wake geometry is reduced to the tip vortices as they mainly contribute to the circulation. Another classical assumption is to consider that the speed of an elementary vortex at the blade tip is equal to the sum of the airflow speed and the average induced velocity on the rotor disk :

$$\vec{v}_o = \begin{bmatrix} \mu \cos \alpha_d \\ 0 \\ \mu \sin \alpha_d + \lambda_{io} \end{bmatrix} = v_o \begin{bmatrix} \sin \chi \\ 0 \\ \cos \chi \end{bmatrix}$$

where v_o is the inflow ratio :

$$v_o = \sqrt{\mu^2 + 2\mu\lambda_{io} \sin \alpha_d + \lambda_{io}^2}$$

Thus, the path of an elementary vortex created at the time t_0 , will be at the time t :

$$x = \cos t_0 + v_0(t - t_0)\sin \chi$$

$$y = \sin t_0$$

$$z = v_0(t - t_0)\cos \chi$$

The tips vortices will be represented by the curves obtained from the previous equations when t_0 varies from $-\infty$ to t . As the inflow ratio is usually small compared with unity, we can approximate the tip vortices by a succession of rings spaced out by a distance of $\Delta h = 2\pi \cdot v_0$ or by a distance of $\Delta h = 2\pi \cdot v_0 / n_b$ if we take into account all the blades (see figures 4 and 5). This approximation is as much true as the inflow ratio is small.

Once the wake geometry has been chosen, we must determine the vortices intensity. On each ring, the circulation has a value varying with the polar angle ξ of the ring referential (see figures 6 and 7). In order to simplify our problem, we will put the vortex intensity in a Fourier expansion depending on ξ . So for the n^{th} ring, we will have :

$$\Gamma^n = \Gamma_0^n + \Gamma_{1c}^n \cos \xi + \Gamma_{1s}^n \sin \xi + \dots$$

To determine the constants Γ and to assure a good compatibility between our wake model and the inflow model used for the computation of the rotor aerodynamic loads, the velocities are matched in the rotor disc plane.

The inflow model is of the form :

$$\lambda_i = \lambda_{i0} + \lambda_{i1c} r \cos \psi + \lambda_{i1s} r \sin \psi$$

where r and ψ are the polar coordinates of the referential of the rotor disc. These formulae give the first coefficients of the Fourier expansion of the induced downwash on the rotor disc. These coefficients are expanded in power series of r at the first order. The same thing is now done with the expression of the velocities induced by the vortex rings on the rotor disc. We will firstly expand these expressions in Fourier series and secondly expand the coefficients of the Fourier expansions in power series of r . By equalizing this last expression to the expression of the inflow model at the rotor disc, we can determine the circulations.

To summarize, the wake model will be determined in four steps:

- Firstly, we determine the analytical expressions of the velocities induced by a vortex ring whose intensity is expanded in a Fourier serie. These expressions depend linearly on the coefficients of the Fourier expansion.

- The second step consists of calculating the velocities induced by all the vortex rings.

- The next step concerns the calculation of the circulations. We expand the expression of the downwash induced by all the vortex rings on the rotor disc and by matching it with the expression of the inflow model used on the rotor disc, we obtain a linear system of the circulations.

- We have obtained now the field of the induced velocities at a given time, for a given position of the blades. The vortex rings move with a velocity v_0 along the wake axis and at each $1/n_b$ rotor turn a new ring is "created". This results in variations of the induced velocities at a given location as much important as this location is close to the rings. As we are only interested in average values of the induced velocities, we will calculate them on a $1/n_b$ rotor turn.

Velocities induced by a vortex ring

The vortex intensity is first expanded in a Fourier serie. The expression of the induced velocities is given by the Biot-Savart law (see figure 6). We obtain for each term of the serie:

$$\Gamma = \Gamma_0$$

$$\lambda_{r0} = \frac{\Gamma_0}{2\pi [z^2 + (1+r)^2]^{1/2}} \left[-K(m) + \frac{[z^2 + r^2 + 1]}{[z^2 + (1-r)^2]} E(m) \right]$$

$$\lambda_{\theta 0} = 0$$

$$\lambda_{z0} = \frac{\Gamma_0}{2\pi [z^2 + (1+r)^2]^{1/2}} \left[K(m) - \frac{[z^2 + r^2 - 1]}{[z^2 + (1-r)^2]} E(m) \right]$$

$$\Gamma = \Gamma_{1c} \cos \xi$$

$$\lambda_{r1c} = \frac{\Gamma_{1c} \cos \theta}{2\pi r^2 [z^2 + (1+r)^2]^{1/2}} \left[-[1 + z^2 + r^2] K(m) + \frac{[1 + r^4 + 2z^2 + 2r^2 z^2 + z^4]}{[z^2 + (1-r)^2]} E(m) \right]$$

$$\lambda_{\theta 1c} = \frac{\Gamma_{1c} \sin \theta}{2\pi r^2 [z^2 + (1+r)^2]^{1/2}} \left[[1 + z^2 + r^2] K(m) - [(1+r)^2 + z^2] E(m) \right]$$

$$\lambda_{z1c} = \frac{\Gamma_{1c} \cos \theta}{2\pi r [z^2 + (1+r)^2]^{1/2}} \left[[z^2 + r^2] K(m) - \frac{[-r^2 + r^4 + z^2 + 2r^2 z^2 + z^4]}{[z^2 + (1-r)^2]} E(m) \right]$$

$$\Gamma = \Gamma_{2c} \cos 2\xi$$

$$\lambda_{r2c} = \frac{\Gamma_{1c} \cos 2\theta}{6\pi r^3 [z^2 + (1+r)^2]^{1/2}} \left[-[2 - r + 2r^2 + 2z^2][2 + r + 2r^2 + 2z^2] K(m) + \frac{[1 + r^2 + z^2][4 - 5r^2 + 4r^4 + 8z^2 + 8r^2 z^2 + 4z^4]}{[z^2 + (1-r)^2]} E(m) \right]$$

$$\lambda_{\theta 2c} = \frac{2\Gamma_{1c} \sin 2\theta}{3\pi r^3 [z^2 + (1+r)^2]^{1/2}} \left[[1 - r + r^2 + z^2][1 + r + r^2 + z^2] K(m) - [1 + r^2 + z^2][(1+r)^2 + z^2] E(m) \right]$$

$$\lambda_{z2c} = \frac{\Gamma_{1c} \cos 2\theta}{6\pi r^2 [z^2 + (1+r)^2]^{1/2}} \left[[-2 + r^2 + 4r^4 + 2z^2 + 8r^2 z^2 + 4z^4] K(m) - \frac{[-2 + 5r^2 - 7r^4 + 4r^6 - r^2 z^2 + 12r^4 z^2 + 6z^4 + 12r^2 z^4 + 4z^6]}{[z^2 + (1-r)^2]} E(m) \right]$$

where :

$$m = \frac{4r}{[z^2 + (1+r)^2]}$$

and K et E are the complete elliptic integrals of the first and second kind.

NB : For circulations of type $\Gamma = \Gamma_{ns} \sin n\xi$, one has only to replace $\cos n\theta$ terms by $\sin n\theta$ and conversely.

To avoid the singularity on the ring ($r=1$), we can use the method developed by Johnson [6] which replaces the vortex ring by a vortex torus of radius r_c for points very close to the

ring. In this case, it is equivalent to multiply the velocities by $d^2/(d^2+r_c^2)$ where d is the distance to the ring.

Total induced velocities

All the previous expressions have been given in the local referential of the ring n . To obtain the velocities induced by all the vortex rings, we must change from the local referential (O, x_n, y_n, z_n) , (O, r_n, θ_n, z_n) to the rotor disc referential (O, x, y, z) , (O, ρ, ψ) (see figures 7 and 8). Therefore :

$$x_n = x - \Delta X_n$$

$$y_n = y$$

$$z_n = z - \Delta Z_n$$

and :

$$m \cos \theta_n = \rho \cos \psi - \Delta X_n$$

$$m \sin \theta_n = \rho \sin \psi$$

$$m^2 = \rho^2 - 2\rho \Delta X_n \cos \psi + \Delta X_n^2$$

where :

$$\Delta X_n = n \Delta h \tan \chi$$

$$\Delta Z_n = n \Delta h$$

Thus, the total velocity is given by :

$$\vec{\lambda}_i = \sum_{n=0}^{N_a-1} (\vec{\lambda}_{i0}(m, \theta_n, z_n) + \vec{\lambda}_{i1c}(m, \theta_n, z_n) + \vec{\lambda}_{i1s}(m, \theta_n, z_n) + \dots)$$

where N_a is the number of vortex rings used for the calculation.

All these terms are proportional to the circulations. So, in order to simplify the notations, we will write :

$$\vec{\lambda}_i = \Gamma \vec{\bar{\lambda}}_i$$

Hence :

$$\vec{\bar{\lambda}}_i = \sum_{n=0}^{N_a-1} (\Gamma_0^n \vec{\bar{\lambda}}_{i0}(m, \theta_n, z_n) + \Gamma_{1c}^n \vec{\bar{\lambda}}_{i1c}(m, \theta_n, z_n) + \Gamma_{1s}^n \vec{\bar{\lambda}}_{i1s}(m, \theta_n, z_n) + \dots)$$

Calculation of the circulation

As the model of Glauert and other models give only the three first coefficients of the expansion, we can take only three constants Γ for the circulation. Moreover, we must limit our expansions to the first harmonics in ψ and to the first order in ρ . One solution is to take the same circulations Γ_0 , Γ_{1c} and Γ_{1s} for all the rings.

By using the expansions described previously, we have obtained at a point $(\rho, 0)$ of the rotor disc, the expansion of the downwash induced by the vortex ring whose center in the rotor disc coordinates is (r, z) :

$$\Lambda_{z,d}(\rho) = \frac{C_0^0(r, z)}{2} + C_0^1(r, z)\rho \cos \Psi + o(\rho^2)$$

$$\Lambda_{z,c}(\rho) = \frac{C_1^0(r, z)}{2} + C_1^1(r, z)\rho \cos \Psi + o(\rho^2)$$

$$\Lambda_{z,s}(\rho) = S_1^1(r, z)\rho \sin \Psi + o(\rho^2)$$

where :

$$C_0[z, z] = \frac{0 \quad (1 - r - z)^2 E[m_0] \quad K[m_0]}{2 \pi \quad \frac{1}{2} \quad \frac{1}{2}} + \frac{1}{2 \pi \quad \frac{1}{2} \quad \frac{1}{2}}$$

$$C_0[z, z] = ((-2 + r + 3r^2 - 2r^3 + r^5 - r^6 + (-4 + 14r^2 - 2r^4)z + (-2 - r - r^2)z^2) E[m_0]) / (2 \pi \quad \frac{1}{2} \quad \frac{1}{2} \quad r) +$$

$$\frac{(2 - r - 3r^2 + r^3 + r^4 + (2 - r + r^2)z^2) K[m_0]}{2 \pi \quad \frac{1}{2} \quad \frac{1}{2} \quad r}$$

$$C_1[r, z] = \frac{0 \quad (-r + r^2 + (1 + 2r)z + z^2) E[m_0] \quad (-r - z) K[m_0]}{2 \pi \quad \frac{1}{2} \quad \frac{1}{2}} + \frac{1}{2 \pi \quad \frac{1}{2} \quad \frac{1}{2}}$$

$$C_1[r, z] = ((3r^2 - r^3 - 6r^4 + 2r^5 + 3r^6 - r^7 + (1 + r - 5r^2 - 5r^4 - r^5 + r^6)z + (3 + 2r - 5r^2 + r^3 + 3r^4)z^2 + (3 + r + 3r^2)z^3 + z^4) E[m_0]) / (2 \pi \quad \frac{1}{2} \quad \frac{1}{2} \quad r) +$$

$$\frac{(-r + r^2 + r^3 - r^4 + (-1 + r + 3r^2 - r^4)z + (-2 + r - 2r^2)z^2 - z^3) K[m_0]}{2 \pi \quad \frac{1}{2} \quad \frac{1}{2} \quad r}$$

$$S_1[r, z] = \frac{1 \quad (r - r^2 + (-1 - 2r)z - z^2) E[m_0] \quad (r + z) K[m_0]}{4 \pi \quad \frac{1}{2} \quad \frac{1}{2}} + \frac{1}{4 \pi \quad \frac{1}{2} \quad \frac{1}{2}}$$

with :

$$dm = (1 - r)^2 + z^2$$

$$dp = (1 + r)^2 + z^2$$

and for the rotor disc ring :

0	1	1
$C_0 = C_1 = S_1 = 1/2$		
0	0	
$C_1 = C_1 = 0$		

The comparison with the rotor disc inflow model gives:

$$\Gamma_0 \sum_{\text{rings}} \frac{(C_0^c(\Delta X_n, -\Delta Z_n) + C_1^c(\Delta X_n, -\Delta Z_n))}{2} + \Gamma_{1c} \sum_{\text{rings}} (C_0^c(\Delta X_n, -\Delta Z_n) + C_1^c(\Delta X_n, -\Delta Z_n)) \rho \cos \psi$$

$$+ \Gamma_{1s} \sum_{\text{rings}} S_1^c(\Delta X_n, -\Delta Z_n) \rho \sin \psi = \lambda_{in} + \lambda_{ic} \rho \cos \psi + \lambda_{is} \rho \cos \psi$$

By identification, we obtain a linear system of the circulations. Two inflow models have been used : the model of Mejer-Drees (Method1) and a variant (Method2) in which there is no cosinusoidal circulation Γ_c . The sinusoidal circulation Γ_s is equal to $-1.5 \Gamma_0$ as provided by the Mejer-Drees model. This allows us to have the intensity of the vortex ring varying quadratically with the distance to the rotor disc.

Average value of the induced velocities

To simplify the calculation and to avoid several computations of the circulations, we can assume that the vortices intensities do not vary much. Hence, if we consider the velocity induced by a ring at a time t and at a point x in the ring local coordinates, at the time $t+\Delta t$ this point will be in the local referential at the location $\vec{x} - \vec{v}_0 \Delta t$. Thus the velocity at the point x at the time $t+\Delta t$ will be the same at the point $\vec{x} + \vec{v}_0 \Delta t$ at the time t . To calculate the average value of the velocities during $1/n_b$ blades turn, it will be equivalent and easier to compute the average value of the velocities at the time t along the segment $(\vec{x}, \vec{x} + \frac{\Delta h}{\cos \chi} \vec{z}')$:

$$\langle \lambda_i \rangle = \frac{1}{\Delta h} \int_{-\Delta h}^0 \lambda_i(x + u \tan \chi, y, z + u) du$$

Implementation

The implementation of the wake model is given figure 26.

Comparison with experimental results

The wake models obtained by Method1 and Method2 and the Coleman - Glauert model have been implemented in a software in order to be compared with experimental results. The models were not directly implemented in a flight mechanics simulation software, but programmed in a distinct software to allow the desired comparisons. Indeed, if the models had been directly incorporated in a simulation software, we would not have been able to distinguish the errors due to the interaction modelisation from errors due to the other parts of the simulation. The inputs of the wake models are the measured values of the advance ratio, rotor disc angle of attack and rotor thrust obtained during the tests. The induced velocities are directly deduced from these inputs.

The results of the comparison are presented on the figures 21 to 25. Airflow deflections obtained from theory and experiment are compared for the test cases mentioned in paragraph 1. The results are rather good concerning the average values of the deflections in all cases. At low advance ratios, the variations of the airflow deflection along the empennage span are very important and are not well reproduced by the models. This is due to the fact that we have only taken into account the tip vortices. Moreover, the quality of the results decreases slightly as the advance ratio increases. This can be explained by the augmentation of the inflow ratio with the helicopter speed thus by the fact that our wake approximation is as less good as the helicopter speed increases. But, at high speed the induced velocities are relatively small and the rotor-horizontal stabilizer interactions are less important than at low speed.

Conclusion

A simple rotor wake model has been developed in order to determine the rotor - horizontal stabilizer interactions on an helicopter. In spite of the apparent complexity of the formulae given in this paper, this model can be programmed in only 200 or 300 lines and easily integrated in a flight mechanics simulation software without major changes and computation time penalties.

The comparison with wind tunnel measurements of the induced downwash at the empennage location shows relatively good results. The validation of the interaction model is continuing with data derived from flight tests.

Bibliography

- [1] R.T.N. Chen : "A survey of non uniform inflow models for rotorcraft flight dynamics and control applications", 15th European Rotorcraft Forum, Amsterdam, september 1989
- [2] R.P. Coleman, A.N. Feingold, C.W. Stempin : "Evaluation of the induced velocity field of an idealized helicopter rotor", NACA ARR L5E10, 1945
- [3] D.M. Pitt, D.A. Peters : "Theoretical prediction of dynamic-inflow derivatives", Vertica, Vol. 5 pp 21 à 34, 1981
- [4] V.E. Baskin, L.S. Vilsgrube, Ye. S. Vozhdoyev, G.I. Maykapar : "Theory of the lifting air-screw", NASA TTF-283, 1976
- [5] J.G. Leishman, Nai-Pei Bi : "Measurements of a rotor flowfield and the effects on a fuselage in forward flight", 16th European Rotorcraft Forum, Glasgow, september 1990
- [6] Johnson W. : "Helicopter theory", Princeton University Press, 1980

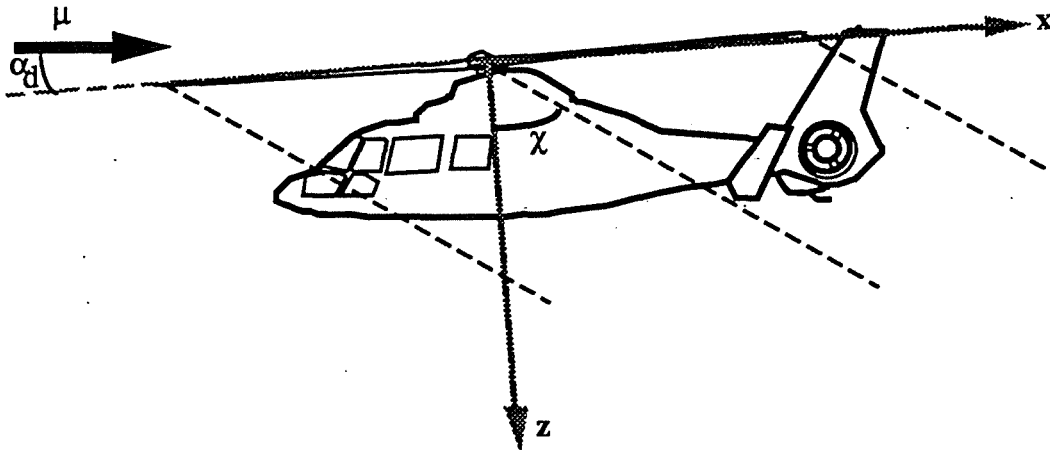


Fig 1 : Rotor disc referential and notations

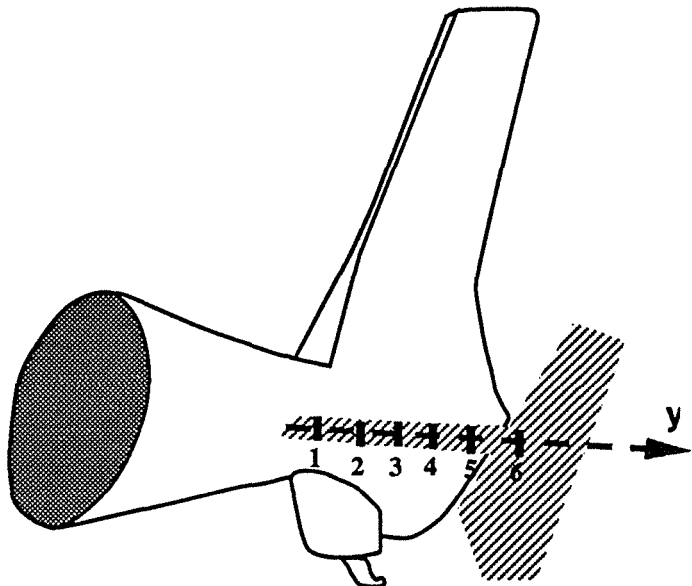


Fig 2 : Measurement points

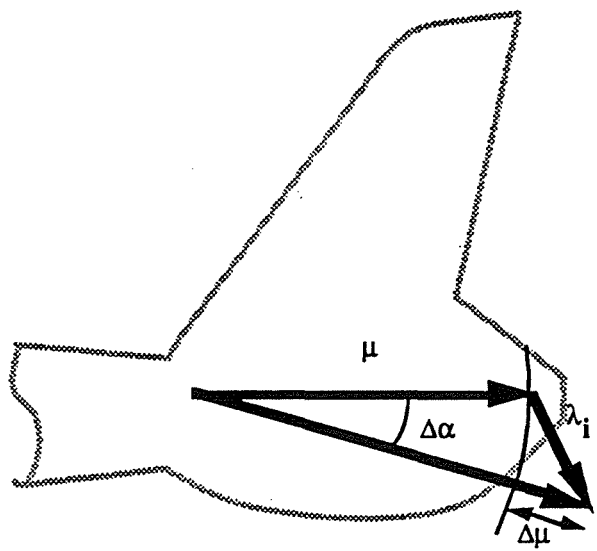


Fig 3 : Induced downwash

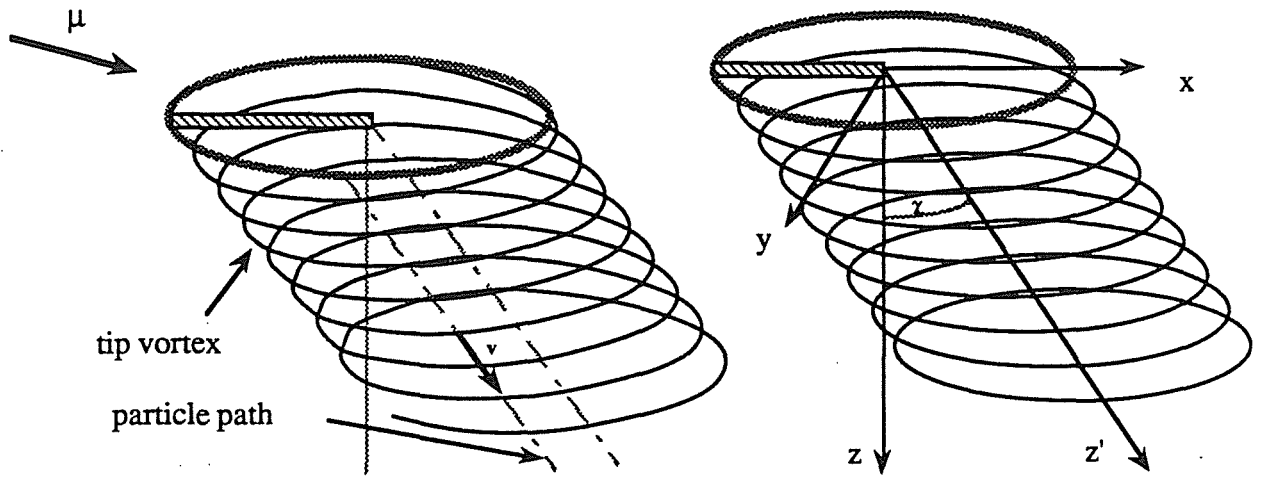


Fig 4 and 5 : approximation of the tip vortices

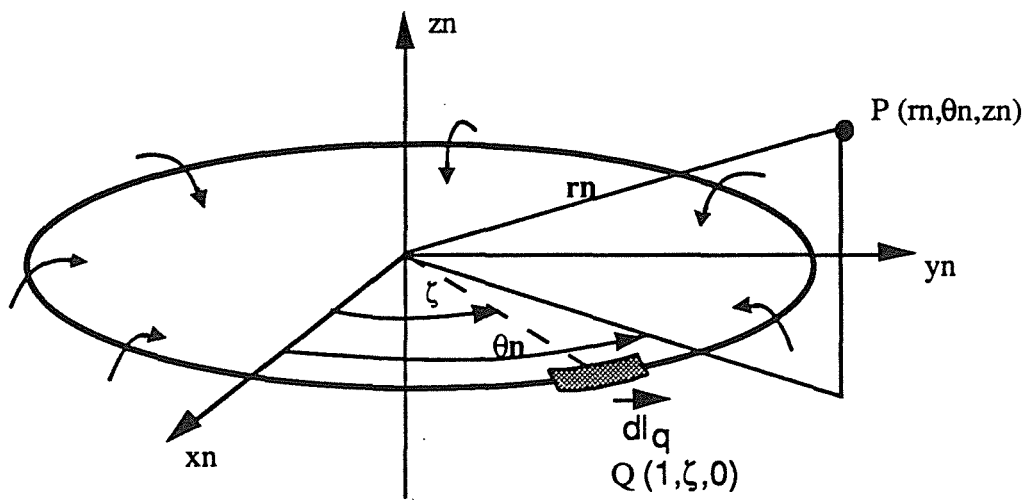


Fig 6 : vortex ring and notations

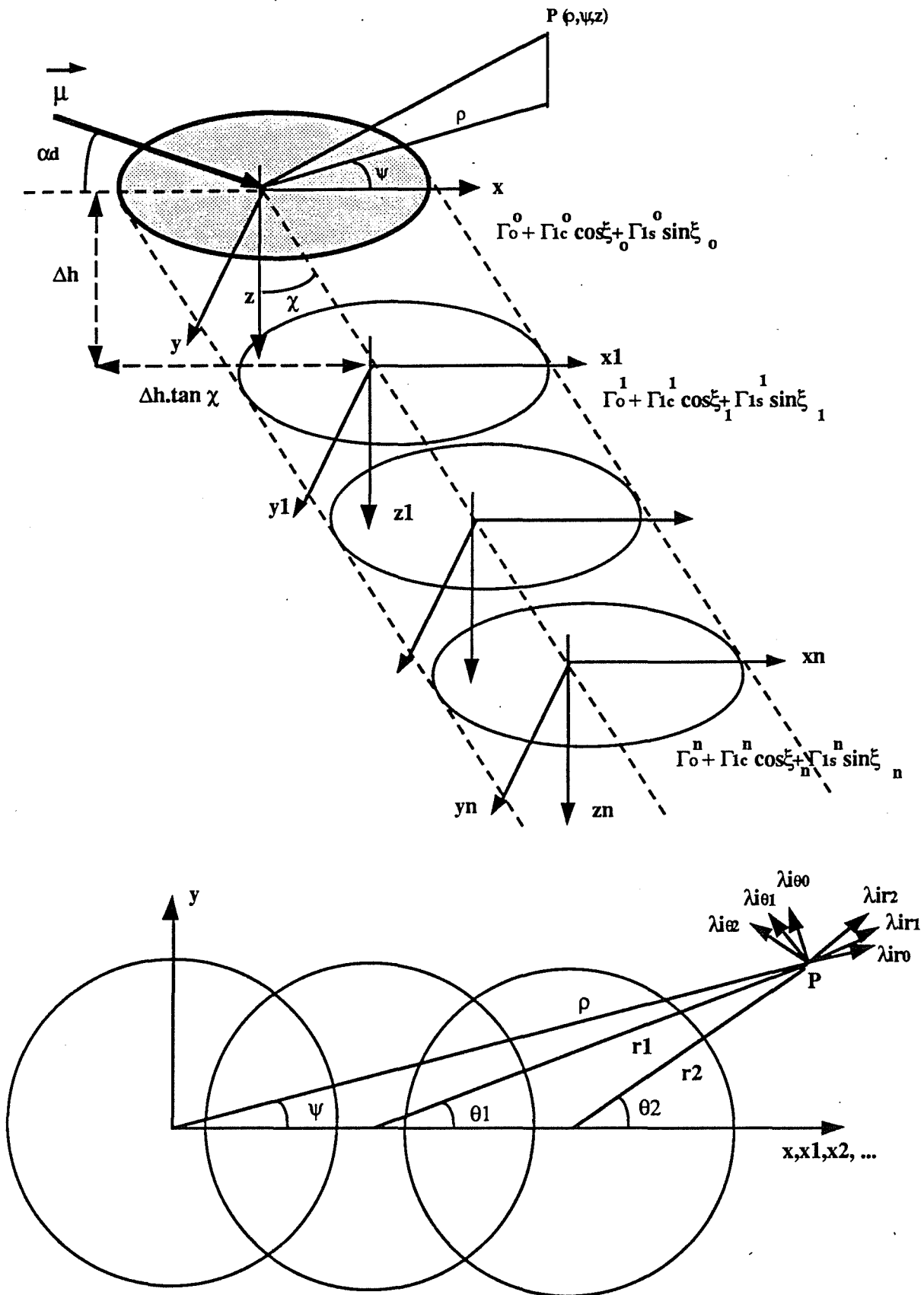
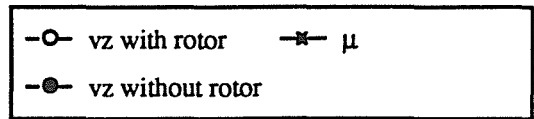
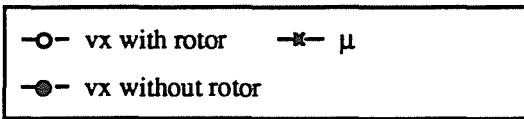
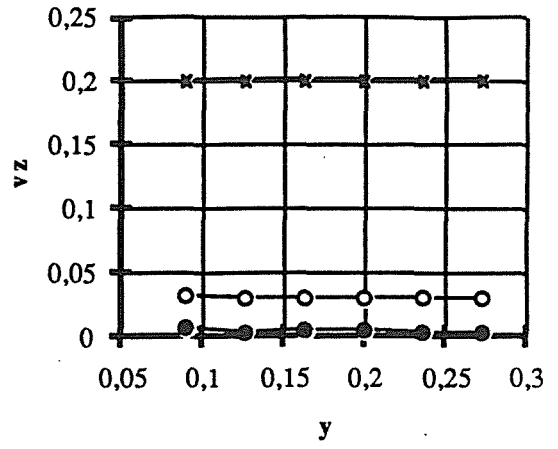
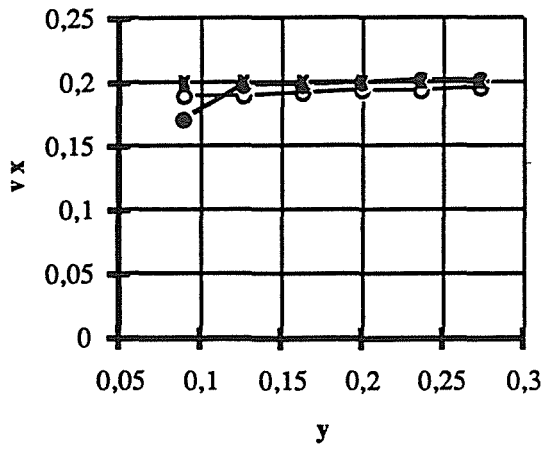
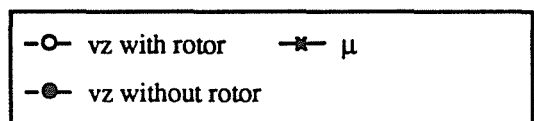
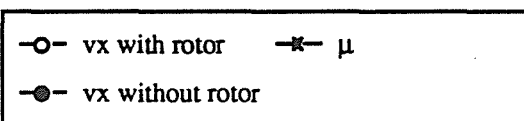
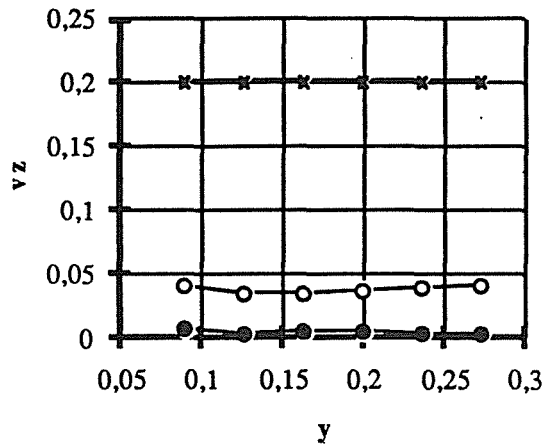
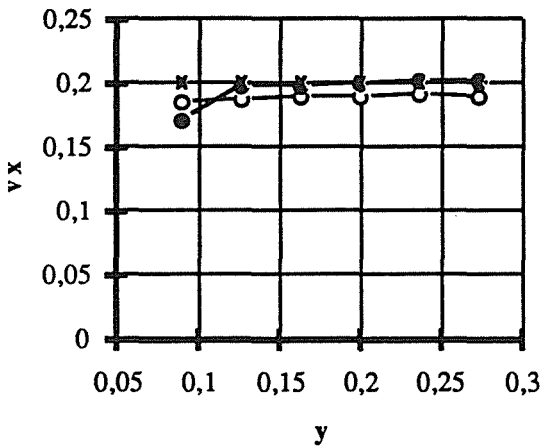


Fig 7 and 8 : Model and notations

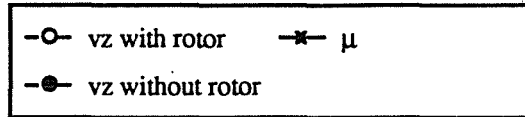
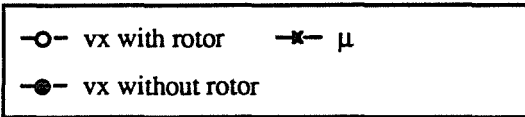
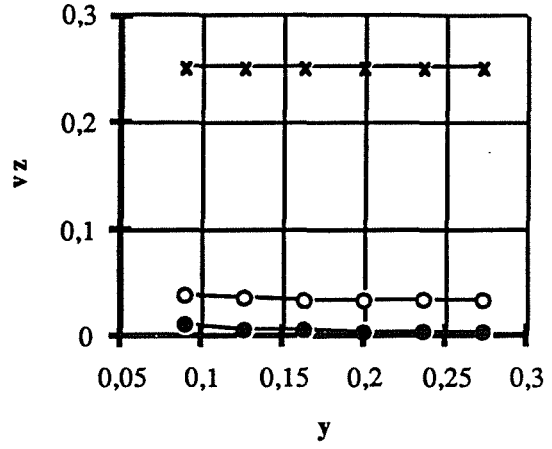
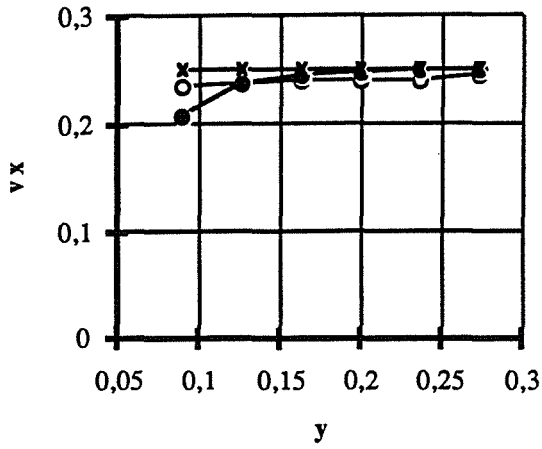


$\mu = 0.20 - mh = 3 \text{ tons}$

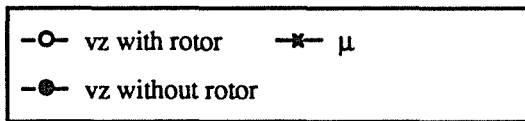
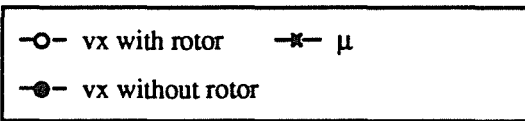
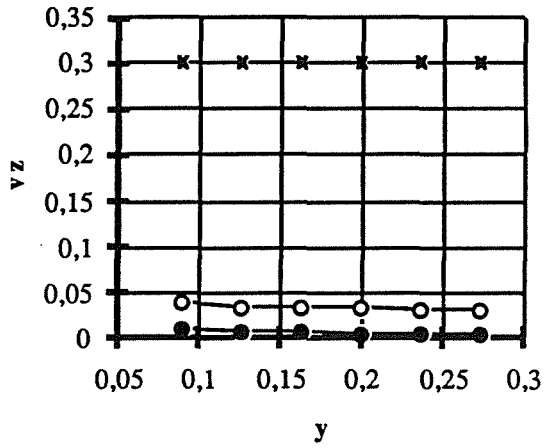
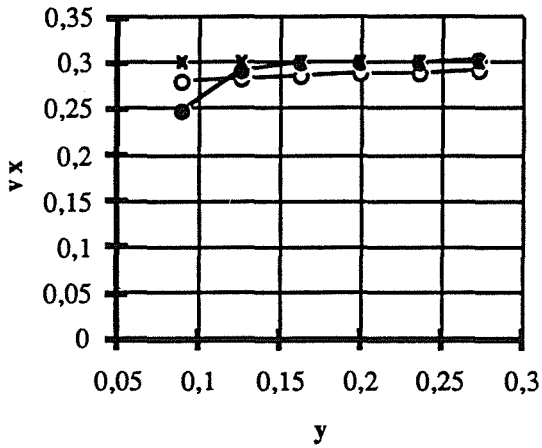


$\mu = 0.20 - mh = 5 \text{ tons}$

Fig 9,10,11 and 12 :
Comparison of tests with and without rotor

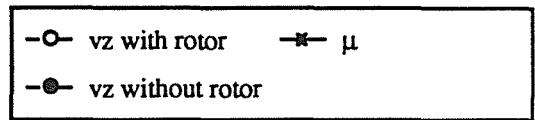
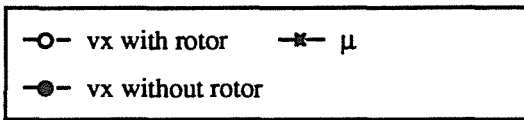
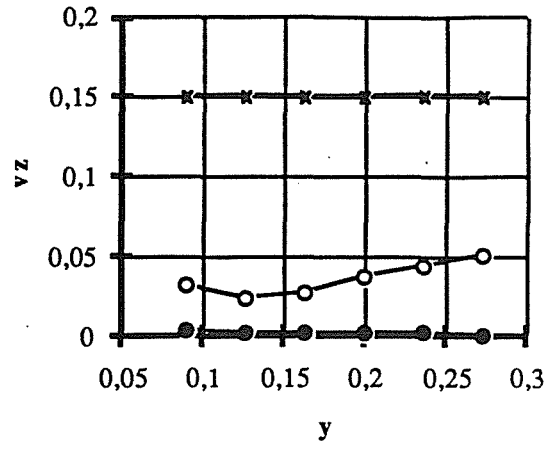
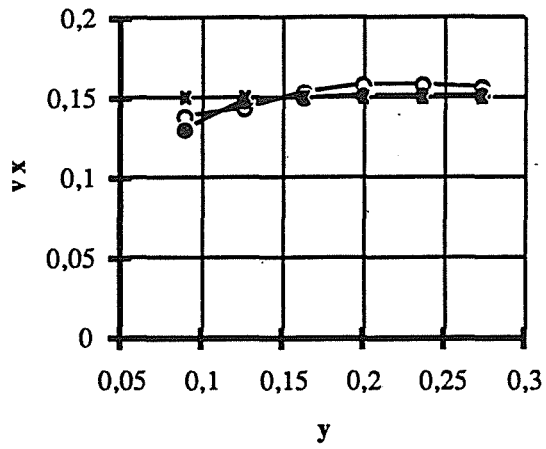


$\mu = 0.25 - mh = 4 \text{ tons}$

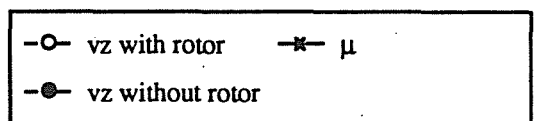
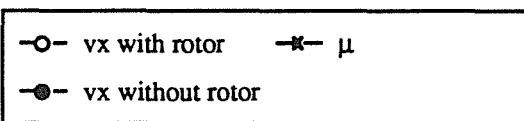
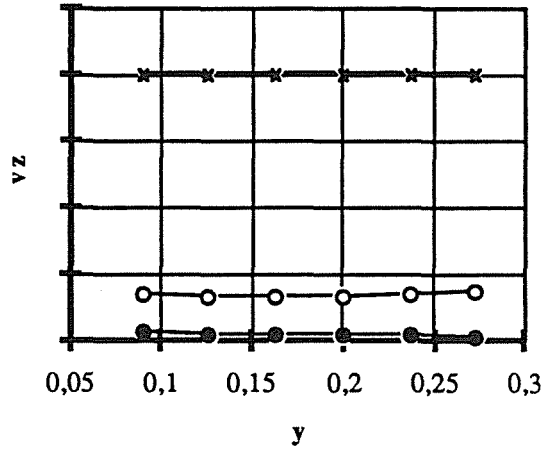
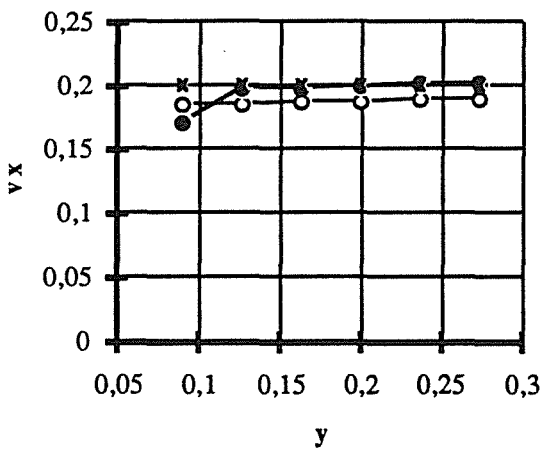


$\mu = 0.30 - mh = 4 \text{ tons}$

**Fig 13,14,15 and 16 :
Comparison of tests with and without rotor**



$\mu = 0.15 - mh = 3 \text{ tons}$



$\mu = 0.20 - mh = 4 \text{ tons}$

Fig 17,18,19 and 20 :
Comparison of tests with and without rotor

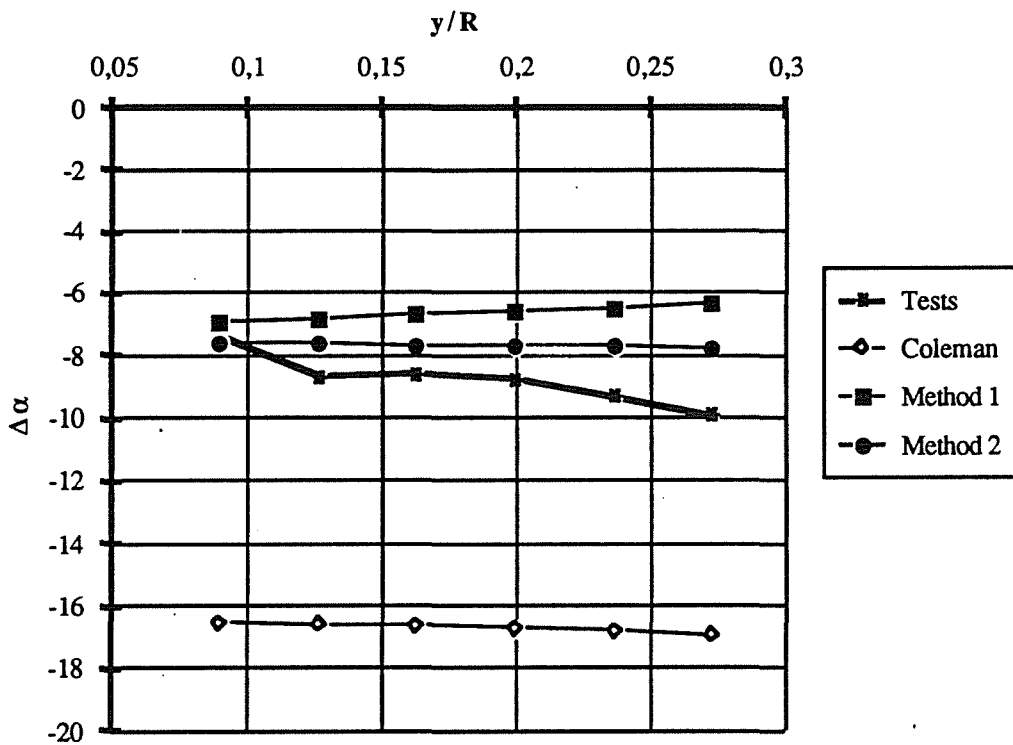
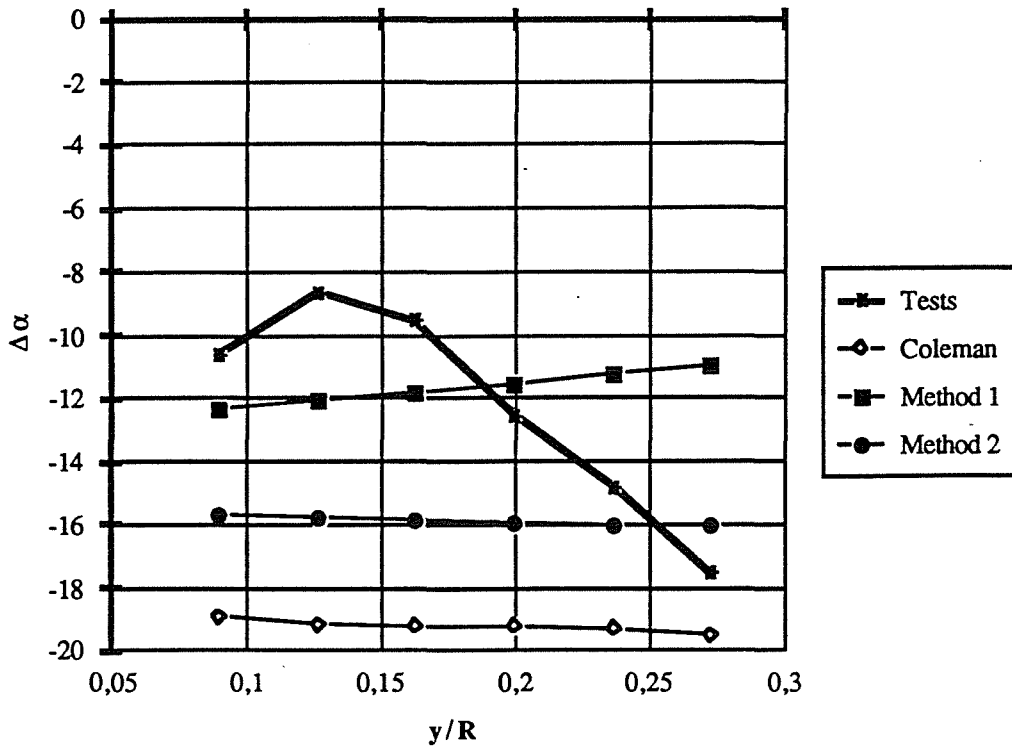


Fig 21 and 22 :
Comparison of measured and computed induced downwash
 $\mu=0,15 - m_h=4t$
 $\mu=0,20 - m_h=4t$

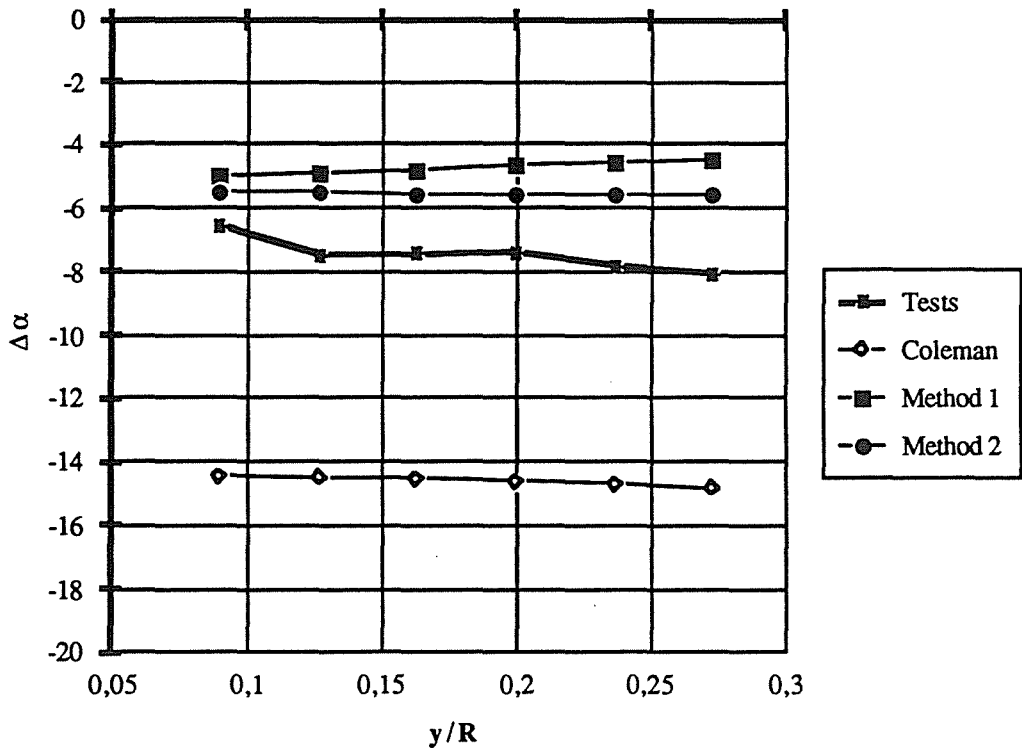
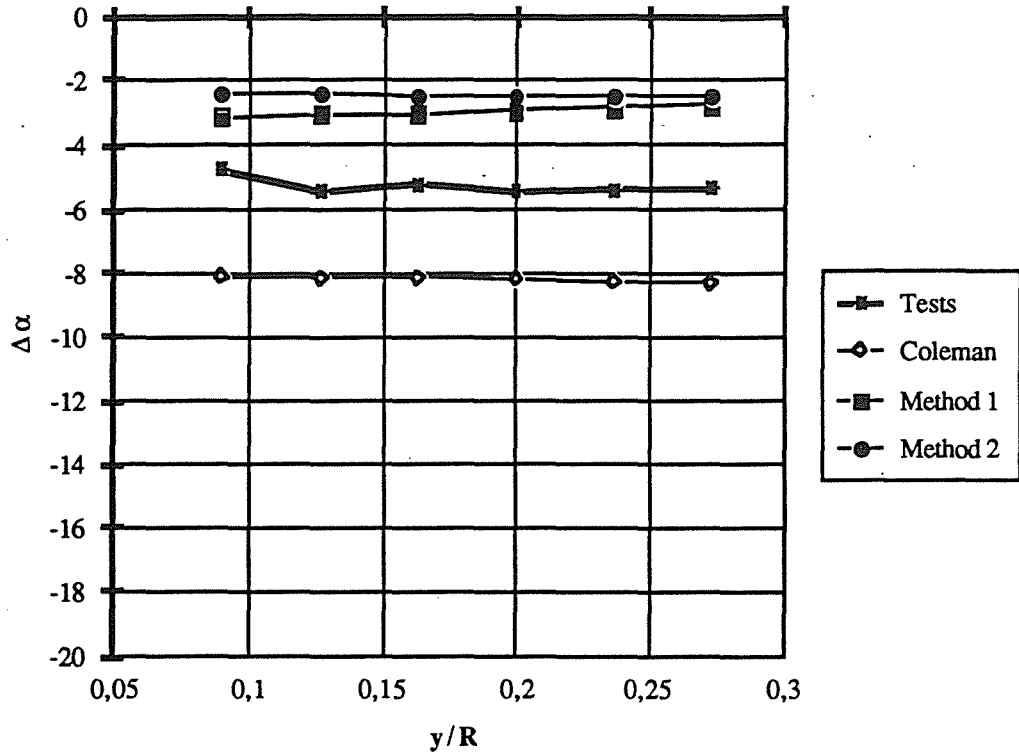


Fig 23 and 24 :
 Comparison of measured and computed induced downwash
 $\mu=0,30 - m_h=4t$
 $\mu=0,20 - m_h=3t$

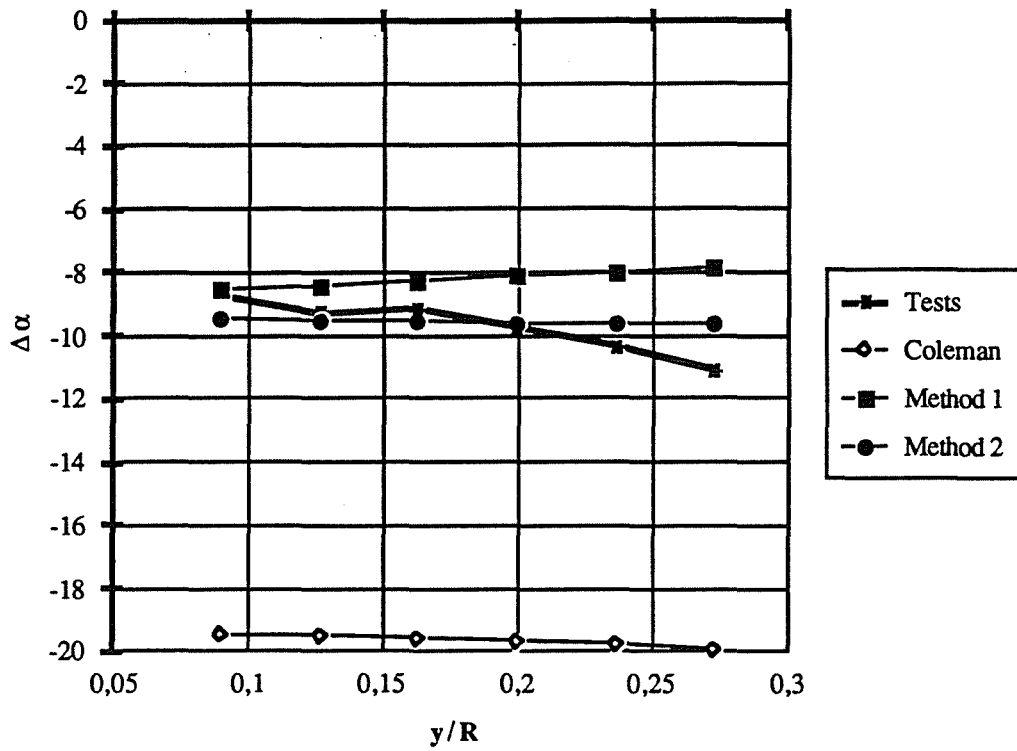


Fig 25 :
Comparison of measured and computed induced downwash
 $\mu=0,20 - m_h=5t$

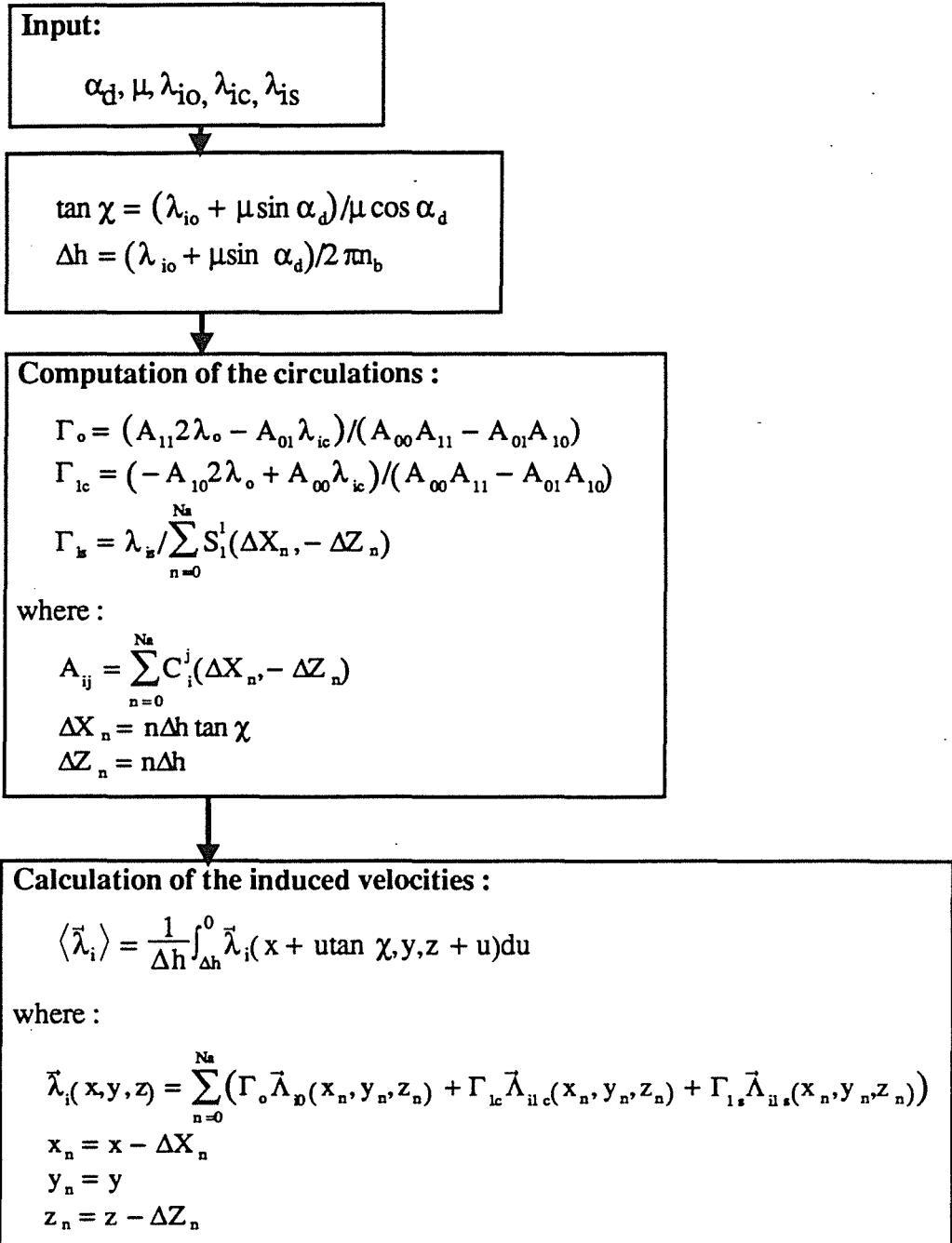


Fig 26 : Implementation of the model